ARTICLES

Effects of three-body forces in the ^{3}H bound state

L. D. Knutson
Physics Department, University of Wisconsin, Madison, Wisconsin 53706

A. Kievsky
Istituto Nazionale de Fisica Nucleare, Sezione de Pisa, I-56100 Pisa, Italy
(Received 2 February 1998)

Calculations of the ^{3}H bound state wave function obtained with the pair-correlated hyperspherical harmonic method are presented for a variety of three-body force models. In each calculation the strength of the three-body force is adjusted to reproduce the observed binding energy. Wave functions obtained with different three-body forces are compared, and results are presented in graphical form for both coordinate and momentum space. For these binding-energy equivalent calculations, the S- and D-state components of the wave function are largely insensitive to the details of the three-body force. However, significant sensitivity is observed for the very small P-state components. [S0556-2813(98)01107-8]

PACS number(s): 21.30.2x, 21.45.1v, 21.60.2n, 27.10.1h

I. INTRODUCTION

The role of three-body forces in nuclear systems is an important and interesting subject. From the theoretical point of view, it is clear that three-body forces must be present at some level. Nucleons have internal structure and consequently they may become polarized in the nuclear environment, and as a result the interaction between any pair may be altered by the presence of a third nucleon. Since polarization effects can be described in terms of virtual excitation of excited states, theoretical models of nuclear three-body forces [1–3] ordinarily begin with pion-exchange diagrams that involve Δ excitation.

While it is clear from the theoretical point of view that three-body forces should be present, experimental evidence that these forces exist is only circumstantial. It is observed that bound state calculations that employ realistic NN poten-

where $\mathbf{x}_i$ and $\mathbf{y}_i$ are the Jacobi coordinates

$$\mathbf{x}_i = \mathbf{r}_j - \mathbf{r}_k \tag{2}$$

and

$$\mathbf{y}_i = (\mathbf{r}_j + \mathbf{r}_k - 2\mathbf{r}_i)/\sqrt{3} \tag{3}$$

with the indices i,j,k cyclic. For the channel decomposition we use LS coupling. The components $\psi(\mathbf{x}_i,\mathbf{y}_i)$ are written as an expansion in channels,

$$\psi(\mathbf{x}_i,\mathbf{y}_i) = \sum_\alpha \psi_\alpha(\mathbf{x}_i,\mathbf{y}_i), \tag{4}$$

where

$$\psi_\alpha(\mathbf{x}_i,\mathbf{y}_i) = \phi_\alpha(x_i,y_i)\mathcal{Y}_\alpha^{jk,i}(\hat{\mathbf{x}}_i,\hat{\mathbf{y}}_i). \tag{5}$$

Here ϕ_α is a function of the radial coordinates x_i and y_i, while the quantity $\mathcal{Y}_\alpha$ is a spin/angle/isospin function constructed in the following coupling scheme:

$$\mathcal{Y}_\alpha^{jk,i} = [(l_x,l_y)L;(s^{jk},s_i)S]_J^{J_z}[t^{jk},t_i]_T^{T_z}. \tag{6}$$

In this expression l_x and l_y represent the orbital angular momentum associated with the coordinates $\mathbf{x}_i$ and $\mathbf{y}_i$, respectively, and L is the total orbital angular momentum. The quantity s^{jk} is the total spin of the pair j,k,

$$\mathbf{s}^{jk} = \mathbf{s}_j + \mathbf{s}_k, \tag{7}$$

and the channel spin $\mathbf{S}$ is the vector sum of $\mathbf{s}^{jk}$ and $\mathbf{s}_i$. The isospin quantum numbers are defined in the analogous way. Even parity is obtained by requiring $l_x + l_y$ to be even, and the final wave function Ψ is fully antisymmetric if the channel wave functions, ψ_α, are antisymmetric under interchange of j and k ($l_x + s^{jk} + t^{jk}$ must be odd).

In place of x_i and y_i it is convenient to employ the hyperradial coordinate

$$\rho = [x_i^2 + y_i^2]^{1/2}. \tag{8}$$

One can easily show that this quantity is just the sum in quadrature of the interparticle separations,

$$\rho^2 = \tfrac{2}{3}(r_{12}^2 + r_{23}^2 + r_{31}^2). \tag{9}$$

Along with ρ we use hyperspherical coordinate z_i defined by the equation

$$z_i = \cos 2\phi_i, \tag{10}$$

where

$$x_i = \rho\cos\phi_i, \quad y_i = \rho\sin\phi_i. \tag{11}$$

With these definitions and parameters, the bound-state wave functions are generated following the procedures outlined in Ref. [10]. The channel expansion of ψ [Eq. (4)] included the 14 basis states listed in Table I. In the table M_α is the number of terms in the hyperspherical expansion of ϕ_α (see Ref. [10]).

The expansion of Ψ in terms of the three Faddeev-like components is an efficient means of generating a fully antisymmetric wave function. However, since the components are expressed in terms of different sets of Jacobi coordinates, the wave function has some peculiar properties. For example, the various terms in the expansion of ψ in channels α are not mutually orthogonal. Thus, for example, there is a nonzero overlap between the $\alpha = 1$ component of ψ_1 and the $\alpha = 9$ component of ψ_2. As a result, with this representation of Ψ there is no natural way to define probability weights for the individual channels.

TABLE I. Quantum numbers of the 14 terms employed in the channel expansion of the wave function $\psi_\alpha(\mathbf{x}_i,\mathbf{y}_i)$. M_α is the number of hyperradial functions used in the expansion of $\phi_\alpha(x_i,y_i)$.

α	l_x	l_y	L	s^{jk}	S	t^{jk}	M_α
1	0	0	0	1	$\frac{1}{2}$	0	8
2	0	0	0	0	$\frac{1}{2}$	1	8
3	2	0	2	1	$\frac{3}{2}$	0	7
4	0	2	2	1	$\frac{3}{2}$	0	7
5	2	2	0	1	$\frac{1}{2}$	0	6
6	2	2	2	1	$\frac{3}{2}$	0	6
7	2	2	1	1	$\frac{1}{2}$	0	6
8	2	2	1	1	$\frac{3}{2}$	0	6
9	1	1	0	1	$\frac{1}{2}$	1	2
10	1	1	1	1	$\frac{1}{2}$	1	3
11	1	1	1	1	$\frac{3}{2}$	1	2
12	1	1	2	1	$\frac{3}{2}$	1	2
13	1	1	0	1	$\frac{1}{2}$	0	2
14	1	1	1	0	$\frac{1}{2}$	0	2

To avoid these complications, the wave function Ψ generated by the method outlined above is rewritten in terms of a single set of Jacobi coordinates. We choose the pair $\mathbf{x}_1$ and $\mathbf{y}_1$, and must therefore transform ψ_2 and ψ_3. When this is done, new wave function components (beyond the 14 included in the original expansion of ψ) are generated.

We then further simplify Ψ by projecting out from the isospin wave functions only those terms in which particle No. 1 is the proton. With this choice the coordinate $\mathbf{x}$ in the projected wave function connects the two identical particles, and as a result, the only channels that survive are those for which $l_x + s^{23}$ is even. In making the isospin projection, the parts of the wave function which one discards are, except for labeling, just copies of the final projected wave function. To restore the normalization integral to unity, the projected wave functions are multiplied by $\sqrt{3}$.

B. Three-body potentials

A number of three-nucleon potentials models have been proposed in the literature. The most commonly used potentials are the Tucson-Melbourne (TM) potential [1,5], the Brazil (BR) potential [2], and the Urbana (UR) potentials [3,4,11]. These potentials are similar in some respects, since they all incorporate the basic 2π-exchange Δ-excitation processes, and all are characterized by a rather complex dependence on the spins, isospins, and coordinates of the three interacting nucleons (see, for example, Ref. [12]). In addition to these interactions, the UR potential contains a purely cen-

tral term with no spin-isospin dependence which is included to give repulsion at short distances.

It has been pointed out in Ref. [9] that the 2π-exchange $3N$

TABLE II. Properties of the lowest S-, P-, and D-state components of the bound state wave function. For state 11 the entry in the D_α column is actually $\tilde{D}_\alpha$ defined in Eq. (25).

α	l_x	l_y	L	s^{jk}	S	P_α (%)				D_α			
						Cent	BR	UR	TM	Cent	BR	UR	TM
						S states							
2	0	0	0	0	$\frac{1}{2}$	88.55	88.17	88.01	88.44	5.491	5.518	5.511	5.526
9	1	1	0	1	$\frac{1}{2}$	0.45	0.44	0.44	0.45	1.102	1.106	1.103	1.108
15	2	2	0	0	$\frac{1}{2}$	1.32	1.33	1.33	1.33	1.638	1.646	1.642	1.649
						P states							
10	1	1	1	1	$\frac{1}{2}$	0.020	0.038	0.037	0.037	2 0.0119	2 0.0129	2 0.0132	2 0.0113
11	1	1	1	1	$\frac{3}{2}$	0.020	0.033	0.031	0.044	0.0102	0.0108	0.0107	0.0107
16	2	2	1	0	$\frac{1}{2}$	0.022	0.038	0.036	0.047	0.0051	0.0055	0.0054	0.0055
						D states							
12	1	1	2	1	$\frac{3}{2}$	5.40	5.76	5.89	5.42	2 0.535	2 0.551	2 0.551	2 0.547
17	1	3	2	1	$\frac{3}{2}$	2.26	2.22	2.25	2.30	0.139	0.138	0.138	0.139
18	3	1	2	1	$\frac{3}{2}$	0.66	0.64	0.65	0.62	2 0.049	2 0.054	2 0.054	2 0.053

that, for experiments that probe the bound state, it will be extremely difficult to find evidence (beyond the binding energy discrepancy) for the existence of three body forces. For the dominant S- and D-state wave functions the three-body force effects are very small. In magnitude, the largest observed shifts are only on the order of 0.03 $\mathrm{fm}^{2\,1/2}$ and occur at small ρ (typically $\rho 5 2$ fm). For the P states, the fractional changes are often substantial, but these components represent only a very small portion of the total wave function. Currently, we have no way of observing the P-state components experimentally; however, the present calculations suggest that if one could devise experiments to measure some property of the P-state components, these experiments could well provide a window for observing three-body force effects.

IV. MOMENTUM SPACE RESULTS

Nuclear reactions that are designed to probe bound state wave functions are often sensitive to wave function properties over a relatively small range of momentum transfers. For this reason, it is useful to have access to wave functions in momentum space.

The momentum space wave function for channel α is given by

$$\Phi_\alpha(\mathbf{k},\mathbf{q}) 5 \left(\frac{1}{2\pi}\right)^3 \int e^{2i\mathbf{k}\cdot\mathbf{x}} e^{2i\mathbf{q}\cdot\mathbf{y}} \psi_\alpha(\mathbf{x},\mathbf{y}) d^3x d^3y. \quad (16)$$

By inserting explicit expression for the spin/angle/isospin functions and expanding the exponentials, one obtains

$$\Phi_\alpha(\mathbf{k},\mathbf{q}) 5 g_\alpha(k,q) \mathcal{Y}_\alpha(\hat{\mathbf{k}},\hat{\mathbf{q}}), \quad (17)$$

where

$$g_\alpha(k,q) 5 \left(\frac{2}{\pi}\right) i^{2(l_x 1 l_y)} 3 \int_0^\infty \int_0^\infty j_{l_x}(kx) j_{l_y}(qy) \phi_\alpha(x,y) x^2 dx y^2 dy. \quad (18)$$

Proceeding as we did in coordinate-space, it is useful to introduce ''hypermomentum'' coordinates Q and ζ. We define

$$Q 5 [k^2 1 q^2]^{1/2} \quad (19)$$

and

$$\zeta 5 \cos 2\theta, \quad (20)$$

where

$$k 5 Q \cos\theta, \quad q 5 Q \sin\theta. \quad (21)$$

Note that in terms of Q, the three-body kinetic energy is simply $\hbar^2 Q^2/M$, where M is the nucleon mass.

For low-energy experiments one is interested in the momentum-space wave functions at very low momentum. The low-momentum behavior of a given channel wave function can be quantified in terms of a single parameter. To see this, we note that if Q is sufficiently small, then k and q are both small, and one can expand the spherical bessel functions of Eq. (18) in a power series. Retaining only the leading term we obtain

$$g_\alpha(k,q) \simeq D_\alpha k^{l_x} q^{l_y} / \beta^{l_x 1 l_y 1 3}, \quad (22)$$

where the low-momentum parameter D_α is given by

$$D_\alpha 5 \frac{1}{(2l_x 1 1)!!} \frac{1}{(2l_y 1 1)!!} \left(\frac{2}{\pi}\right) i^{2(l_x 1 l_y)} \beta^{l_x 1 l_y 1 3} 3 \int_0^\infty \int_0^\infty x^{l_x 1 2} y^{l_y 1 2} \phi_\alpha(x,y) dx dy. \quad (23)$$

In these equations we have defined $\hbar^2\beta^2/M 5 B$, where B is the ^{3}H binding energy, and have incorporated appropriate factors of β to make D_α dimensionless.

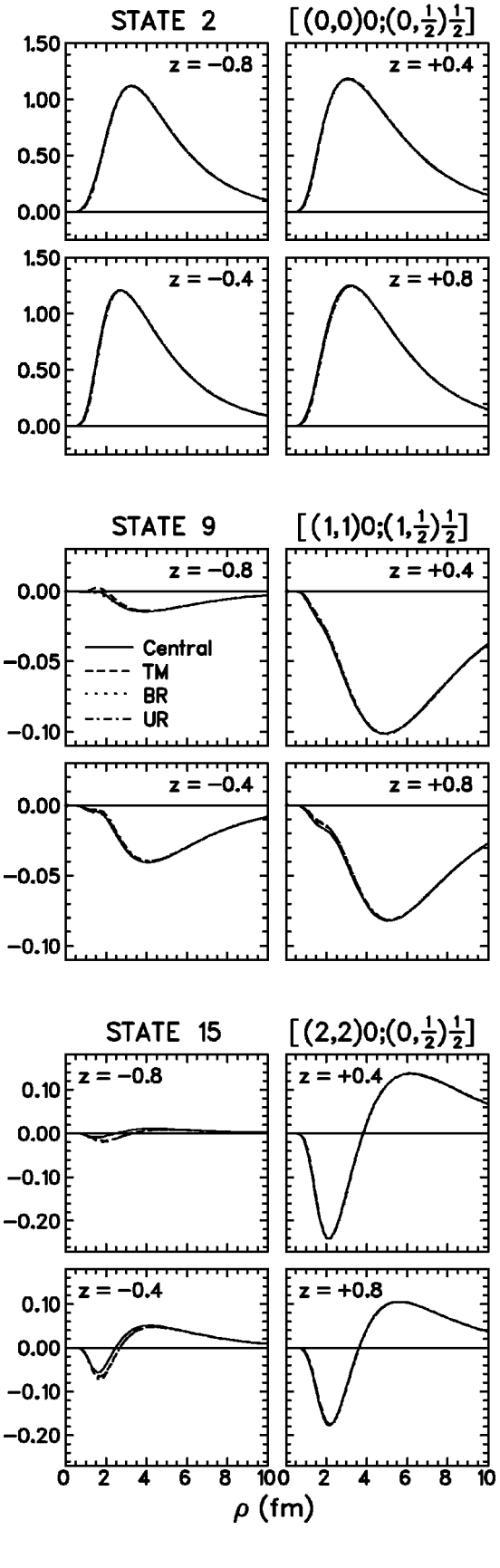

FIG. 1. Calculated S-state components of the ^{3}H wave function plotted as a function of the hyperradius. The quantity shown is $\rho^{5/2}\phi_\alpha(\rho,z)$. The quantum numbers $[(l_x,l_y)L;(s^{jk},s_i)S]$ of each state are indicated in the figure.

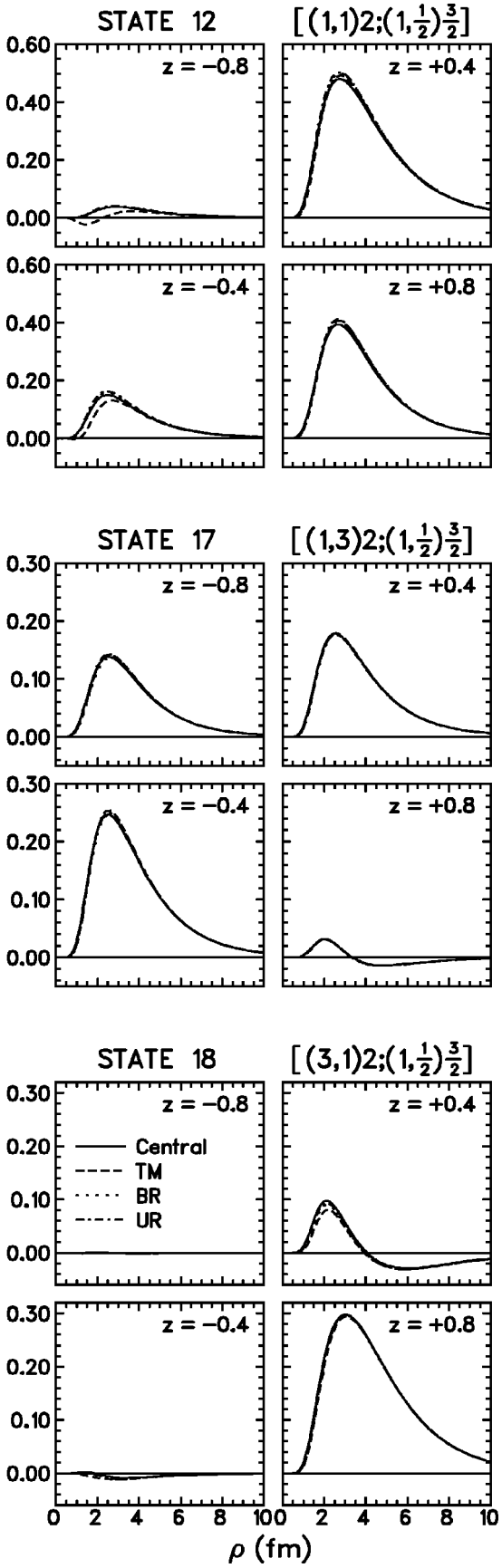

FIG. 2. Calculated D-state components of the ^{3}H wave function plotted as a function of the hyperradius. The quantity shown is $\rho^{5/2}\phi_\alpha(\rho,z)$. The quantum numbers $[(l_x,l_y)L;(s^{jk},s_i)S]$ of each state are indicated in the figure.

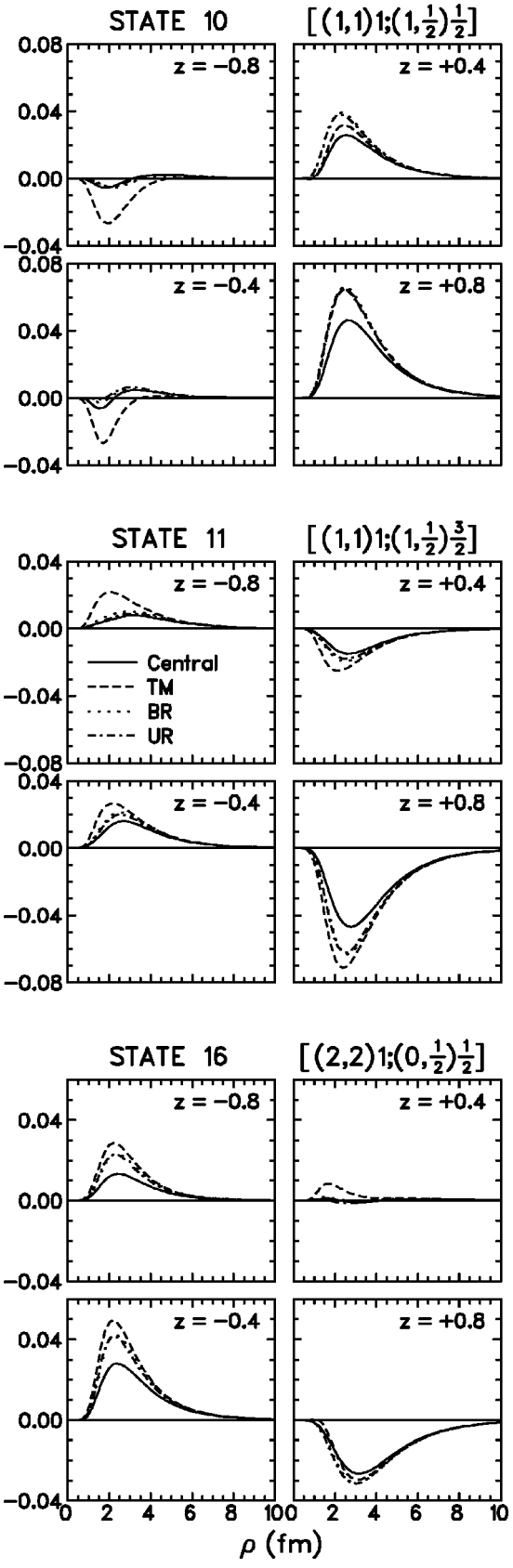

FIG. 3. Calculated P-state components of the ^{3}H wave function plotted as a function of the hyper-radius. The quantity shown is $\rho^{5/2}\phi_\alpha(\rho,z)$. The quantum numbers $[(l_x,l_y)L;(s^{jk},s_i)S]$ of each state are indicated in the figure.

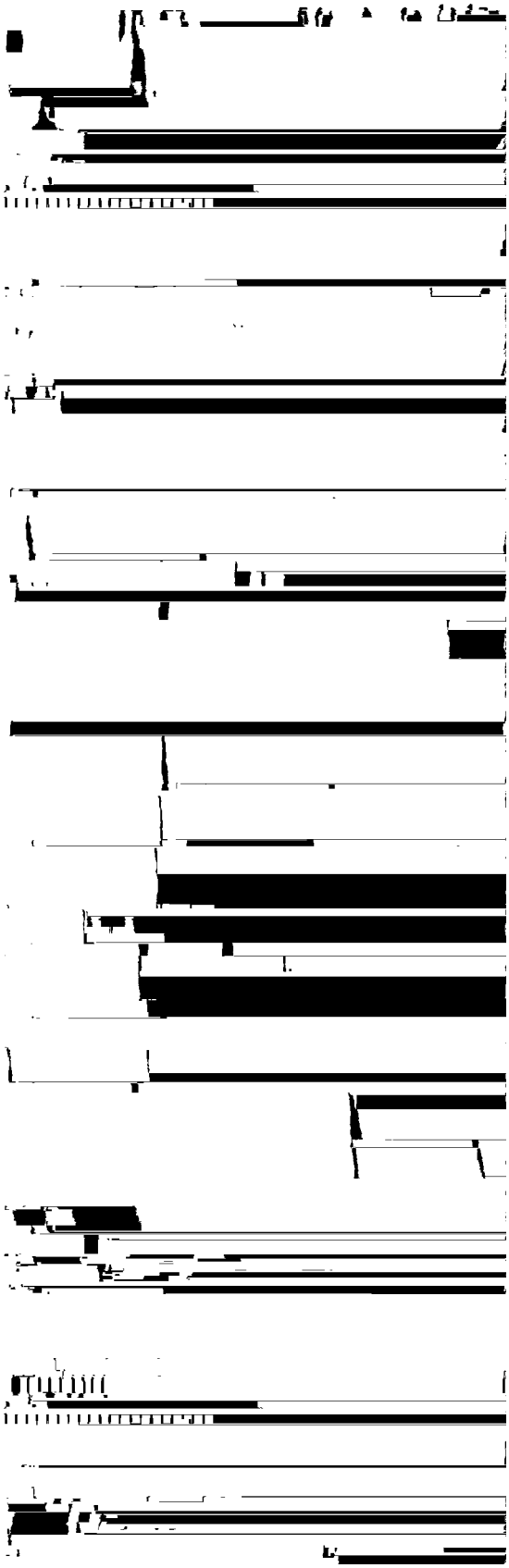

FIG. 4. S-state components of the momentum-space ^{3}H wave functions. The hypermomentum variables Q and ζ are defined in Eqs. (19) and (20). The quantity shown in the plots is $Q^{5/2}g_\alpha(Q,\zeta)$. The quantum numbers $[(l_x,l_y)L;(s^{jk},s_i)S]$ of each state are indicated in the figure.

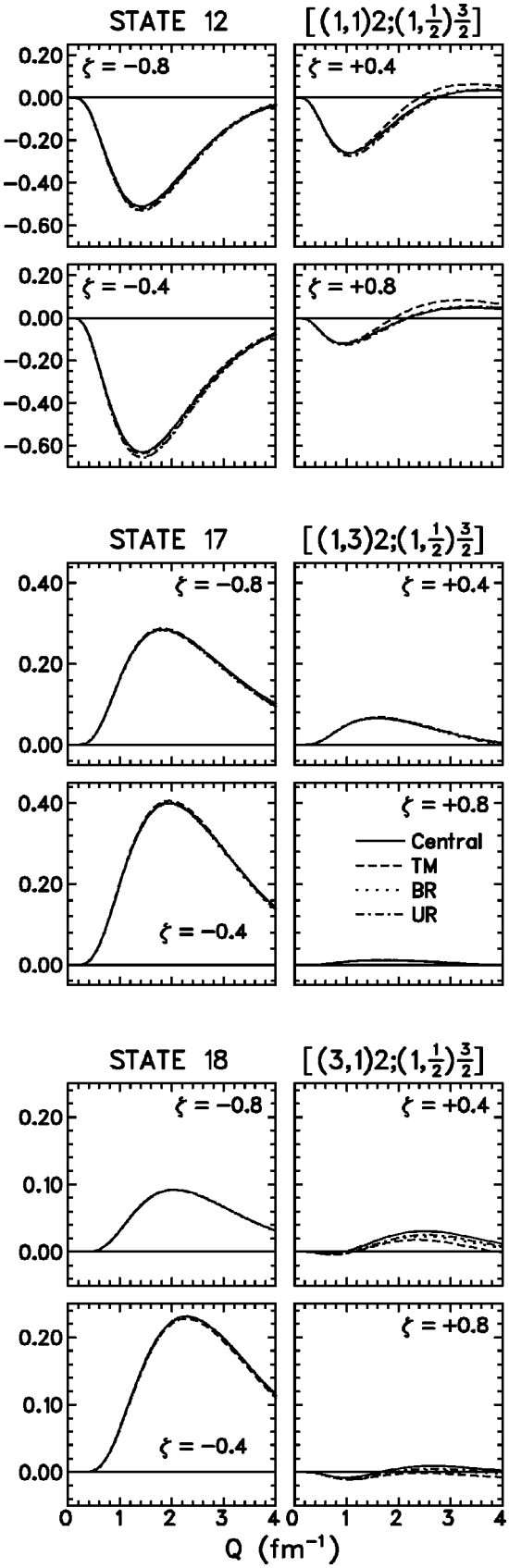

FIG. 5. D-state components of the momentum-space ^{3}H wave functions. The hypermomentum variables Q and ζ are defined in Eqs. (19) and (20). The quantity shown in the plots is $Q^{5/2}g_\alpha(Q,\zeta)$. The quantum numbers $[(l_x,l_y)L;(s^{jk},s_i)S]$ of each state are indicated in the figure.

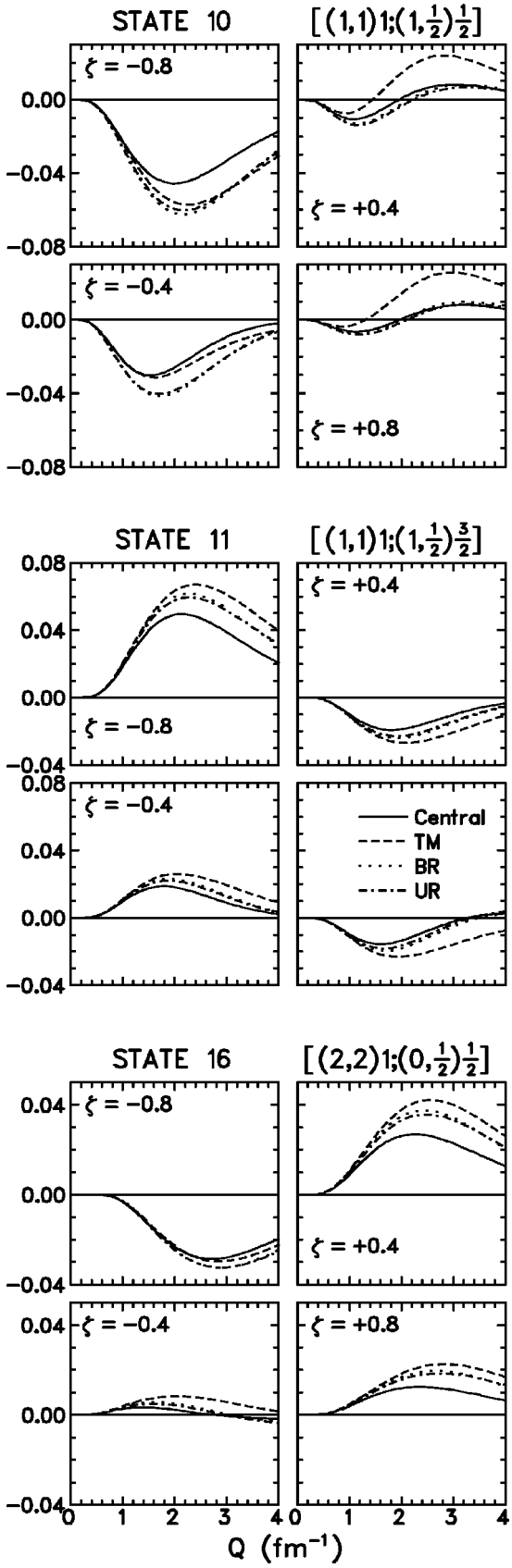

FIG. 6. P-state components of the momentum-space ^{3}H wave functions. The hypermomentum variables Q and ζ are defined in Eqs. (19) and (20). The quantity shown in the plots is $Q^{5/2}g_\alpha(Q,\zeta)$. The quantum numbers $[(l_x,l_y)L;(s^{jk},s_i)S]$ of each state are indicated in the figure.

The state $\alpha = 11$ (see Table I) has a special symmetry property which causes D_α to be zero. State 11 is the ^4P state with $l_x = l_y = 1$. The spin wave function of this state is symmetric under particle interchanges and the angular wave function is antisymmetric. As a result the combined radial-isospin wave function must be symmetric, and this imposes a symmetry on $\phi_\alpha(x,y)$, causing the integral of Eq. (23) to be zero. As a result, for state 11 one finds that the leading term in the momentum expansion is

$$g_\alpha(k,q) \simeq \tilde{D}_\alpha kq(k^2 + q^2)/\beta^7, \tag{24}$$

where

$$\tilde{D}_\alpha = \frac{1}{20}\frac{1}{(2l_x+1)!!}\frac{1}{(2l_y+1)!!} \left(\frac{2}{\pi}\right) i^{-2(l_x+l_y)}\beta^{l_x+l_y+5}\int_0^\infty\int_0^\infty x^{l_x+2}y^{l_y+2}(x^2+y^2) \phi_\alpha(x,y)\,dx\,dy. \tag{25}$$

The D_α values for the various wave functions are given in Table II. As we would expect, the low-momentum parameters for the S- and D-state components are largely insensitive to the $3N$ force. For the S states the parameters vary by less than 1%. For the D states the changes are somewhat larger, but still only on the order of 2–3 % for the dominant component (state 12). For the P states, the low-momentum parameters generally increase, when the purely central $3N$ force is replaced one of the more realistic interactions, but still the changes are only 5–10 %. This result suggests that in experiments to probe the bound-state wave functions, one can not expect to find large sensitivities to the three-body force at low energies, even if one could manage to identify observables that were sensitive to the P-state components.

Finally, in Figs. 4–6 we present the full momentum-space wave functions. As in Figs. 1–3, the channel wave functions

[6] H. Witała, D. Hüber, and W. Glöckle, Phys. Rev. C **49**, R14 (1994).
[7] H. Patberg *et al.*, Phys. Rev. C **53**, 1497 (1996).
[8] J. Zejma *et al.*, Phys. Rev. C **55**, 42 (1997).
[9] L. D. Knutson, Phys. Rev. Lett. **73**, 3062 (1994).
[10] A. Kievsky, M. Viviani, and S. Rosati, Nucl. Phys. **A551**, 241 (1993).
[11] R. B. Wiringa, Phys. Rev. C **43**, 1585 (1991).
[12] C. R. Chen, G. L. Payne, J. L. Friar, and B. F. Gibson, Phys. Rev. C **33**, 1740 (1986).
[13] R. B. Wiringa, R. A. Smith, and T. L. Ainsworth, Phys. Rev. C **29**, 1207 (1984).